Crystal Structure of the Anticancer Drug Cisplatin Bound to Duplex DNA

Patricia M. Takahara,[†] Christin A. Frederick,[‡] and Stephen J. Lippard*,[†]

Contribution from the Department of Chemistry, Massachusetts Institute of Technology, Cambridge, Massachusetts 02139, and Department of Biological Chemistry and Molecular Pharmacology, Dana-Farber Cancer Institute, 44 Binney Street, Boston, Massachusetts 02115

Received July 19, 1996[⊗]

Abstract: The X-ray crystal structure of d(CCTCTG*G*TCTCC)·d(GGAGACCAGAGG), where G*G* represents the major adduct of the antitumor drug cisplatin on a duplex DNA dodecamer, was solved to a resolution of 2.6 Å ($R = 0.203$, R-free $= 0.245$). The molecule crystallizes in the space group $P1$, with unit cell dimensions $a = 31.27$ Å, $b = 35.46$ Å, $c = 47.01$ Å, $\alpha = 79.81°$, $\beta = 84.75°$, $\gamma = 82.79°$, and $Z = 2$. Two molecules in the asymmetric unit are related by a local two-fold symmetry axis and have very similar structures. The duplexes are bent significantly, each having a 26° roll toward the major groove at the site of the platinum intrastrand cross-link. The platinum atom binds to the N7 atoms of adjacent guanine residues, compacting the major groove and widening and flattening the minor groove. Because of the shallow roll, the platinum atom is displaced from the planes of the guanine bases by ∼1 Å and is considerably strained. The overall structure of the cisplatin-modified duplex contains an unusual juxtaposition of A-like and B-like helical segments. This bent structure is accommodated by an interesting and novel packing arrangement in the crystal. One end of each duplex packs end-to-end with another, as in crystal structures of B-DNA, whereas the other end packs into the minor groove of an adjacent molecule, much like A-DNA crystal packing. An unusual backbone-to-backbone packing interaction involving several CH···O hydrogen bonds was also observed. The widened minor groove and the bend caused by platinum binding resembles the DNA component of the structure of the HMG domains of SRY bound to its recognition site DNA. This similarity suggests how HMG-domain proteins might recognize cisplatin−DNA adducts.

Introduction

Cisplatin, or *cis*-diamminedichloroplatinum(II) (*cis*-DDP), is an anticancer drug widely used to treat a variety of tumors, especially those of the testes, ovaries, head, and neck.[1] Several lines of investigation point to deoxyribonucleic acid (DNA) as the most likely biological target associated with the antitumor activity.[2] Cisplatin forms many kinds of DNA adducts, the most prevalent being those in which platinum links N7 atoms of adjacent purine bases.[3] When cisplatin is allowed to react with DNA in vitro, ∼90% of the adducts formed are 1,2-intrastrand cross-links, where platinum coordinates to two adjacent guanine residues or an adjacent adenine and guanine. The remaining are other intrastrand cross-links, interstrand cross-links, monofunctional adducts, or protein−DNA cross-links.[4,5] The 1,2-intrastrand cross-links are of particular interest since they correlate with the clinical efficacy of the drug[6] and are uniquely recognized by cellular proteins which contain a region of about 80 amino acids known as the high mobility group (HMG) domain.[7,8] HMG-domain proteins bind to intrastrand *cis*-[Pt(NH$_3$)$_2$\{d(GpG)\}] and cis-[Pt(NH$_3$)$_2$\{d(ApG)\}] adducts in a structure-specific manner and may potentiate the antitumor activity of the drug by interfering with cellular repair processes.[9,10] It is therefore of interest to understand the detailed molecular structures of cisplatin−DNA adducts and how these structures correlate with HMG-domain protein binding and otherwise alter DNA function.

When *cis*-[Pt(NH$_3$)$_2$(H$_2$O)$_2$]$^{2+}$ interacts with duplex DNA, significant disruptions in base stacking must occur in order to accommodate the coordination requirements of the square-planar platinum(II) atom. In an attempt to understand such structural perturbations several crystallographic studies have been undertaken.[11] The first was an attempt to soak cisplatin into crystals of the self-complementary B-DNA dodecamer d(CGCGAATTCGCG).[12] In this work, three of the eight guanine residues, G4, G10, and G16, appeared to have some affinity for cisplatin but none of the platinum sites in the crystal was fully occupied. Crystal structures with three different levels of cisplatin substitution were solved, and results for the most occupied platinum site, near the N7 atom of residue G16, were analyzed. The crystals had platinum−G16(N7) bond lengths of 2.51, 2.43, and 2.16 Å with occupancies of 20%, 38%, and 61%, respectively. Attempts to obtain more highly substituted platinum sites resulted in crystal degradation. The authors reasoned, from a linear plot of bond length versus percent substitution, that the platinum−N7 bond length would be 1.8 Å at 100% occupancy.

[†] Department of Chemistry, Massachusetts Institute of Technology.
[‡] Department of Biological Chemistry and Molecular Pharmacology, Harvard Medical School.
[⊗] Abstract published in *Advance ACS Abstracts,* November 15, 1996.

(1) Comess, K. M.; Lippard, S. J. In *Molecular Aspects of Anticancer Drug-DNA Interactions*; Neidle, S., Waring, M., Eds.; MacMillan: London, 1993; p 134.
(2) Lippard, S. J. *Science* **1982**, *218*, 1075.
(3) Sherman, S. E.; Gibson, D.; Wang, A. H.-J.; Lippard, S. J. *Science* **1985**, *230*, 412.
(4) Fichtinger-Schepman, A. M. J.; van der Veer, J. L.; den Hartog, J. H. J.; Lohman, P. H. M.; Reedijk, J. *Biochemistry* **1985**, *24*, 707.
(5) Eastman, A. *Biochemistry* **1986**, *25*, 3912.
(6) Reed, E.; Ozols, R. F.; Tarone, R.; Yuspa, S. H.; Poirer, M. C. *Carcinogenesis* **1988**, *9*, 1909.
(7) Pil, P. M.; Lippard, S. J. *Science* **1992**, *256*, 234.
(8) Whitehead, J. P.; Lippard, S. J. In *Metal Ions in Biological Systems*; Sigel, H., Sigel, A., Eds.; Marcel Dekker: New York, 1995; p 687.
(9) Huang, J.-C.; Zamble, D. B.; Reardon, J. T.; Lippard, S. J.; Sancar, A. *Proc. Natl. Acad. Sci. U.S.A.* **1994**, *91*, 10394.
(10) Zamble, D. B.; Mu, D.; Reardon, J. T.; Sancar, A.; Lippard, S. J. *Biochemistry* **1996**, *35*, 10004.
(11) Sherman, S. E.; Lippard, S. J. *Chem. Rev.* **1987**, *87*, 1153.
(12) Wing, R. M.; Pjura, P.; Drew, H. R.; Dickerson, R. E. *EMBO J.* **1984**, *3*, 1201.

S0002-7863(96)02507-3 CCC: $12.00

This study yielded no information about the biologically more relevant bifunctional adducts

The structure of *cis*-[Pt(NH_3)$_2${d(pGpG)-N7(G_1),-N7(G_2)}] has been probed on short segments of single-stranded DNA by X-ray crystallography.[3,13,14] These studies showed platinum coordination at the N7 positions of adjacent guanine bases with concomitant destacking to afford a dihedral angle of about 80° between the planes of the guanine rings, alteration of the sugar pucker of the 5′ nucleotide to a C3′-endo conformation, and hydrogen bond formation between an ammine on the platinum atom and a phosphate oxygen 5′ to the platinum lesion.[3] Because single-stranded DNA molecules lack the constraints of base stacking and Watson−Crick hydrogen bonding, further crystallographic studies of specific platinum adducts were carried out on segments of duplex DNA.

Attempts to characterize such a site-specific cross-link on duplex DNA by single-crystal X-ray methods were undertaken in our laboratory several years ago.[15] In particular, the self-complementary dodecamer DNA oligonucleotide d(GCTG*G*TTAACCA) having an intrastrand *cis*-{Pt(NH_3)$_2$}$^{2+}$ cross-link at the G*G* site was synthesized, purified, and annealed to afford a duplex with two cisplatin cross-links per turn of helix. The platinum adducts were strategically placed such that the bends in each helical turn would be ∼180° apart. The annealed duplex DNA also had a 5′ GC overhang at each end for base pairing with the 5′ ends of neighboring helixes. The bend placements and overhangs were designed to create a structure which was effectively a long and continuous, albeit curved, helix which might pack well in crystals. Crystals with a flat platelike morphology were obtained but diffracted poorly. An analogous sequence, d(ATTG*G*TTAACCA), was also synthesized, purified, annealed, and crystallized. Again, the crystals diffracted poorly and were not suitable for study by X-ray crystallography.

Further attempts to obtain diffraction quality crystals of an intrastrand cisplatin cross-link on duplex DNA involved a more conventional approach. Oligonucleotides with a single GG site for platination were synthesized. In order to increase the yield of purified product, no purines other than the GG target site were present in the strand to be platinated. The pure platinated oligonucleotide was then annealed to its purified, complementary strand to form duplex DNA with a single intrastrand cisplatin 1,2-cross-link. Of the many different sequences examined, only one, d(CCTCTG*G*TCTCC)·d(GGAGACCAGAGG), was of sufficient quality for the X-ray structure to be solved and only after the crystals were allowed to grow slowly for periods of 9−12 months. Several brominated derivatives were obtained for use in multiple isomorphous replacement (MIR) studies, one of which diffracted to 2.6 Å. Data from this crystal were used to obtain the structural parameters described in this report.

The sequence and numbering scheme for this oligonucleotide are given below, where U*3 is 5-bromouridine and platinum binds to the N7 atoms of G*6 and G*7. We hereafter designate

```
5'-C1 -C2 -U*3-C4 -T5 -G*6-G*7-T8 -C9 -T10-C11-C12-3'
3'-G24-G23-A22-G21-A20-C19-C18-A17-G16-A15-G14-G13-5'
```

the ends of this double helix as the 3′ and 5′ ends, where the numbers refer to the platinated strand. A preliminary report of this structure has been published.[16] In the present article, we present a detailed description and analysis of the structure, which illustrates how a segment of platinated DNA can flex to accommodate the 1,2-intrastrand cross-link and reveals packing interactions in the crystal lattice which provide insight into how a cisplatin-modified duplex might come in close contact with other biomolecules. We also compare our results with the investigations of cisplatin-modified duplex DNA by gel electrophoretic[17−19] and NMR spectroscopic techniques.

Experimental Section

Materials. Phosphoramidites and reagents for DNA synthesis were purchased from Cruachem and Glen Research. Crystallization reagents were obtained from Fluka or Aldrich. *cis*-Diamminedichloroplatinum(II) was a gift from the Johnson-Matthey. Reverse phase C4 and C18 high-performance liquid chromatography (HPLC) columns were purchased from Vydac, and ion exchange HPLC columns were obtained from Dionex.

Large-scale HPLC was performed on a Waters 600E pumping system with either a Waters 486 or Waters 484 ultraviolet detector set at 260 nm. Analytical HPLC was done by using a Perkin-Elmer Series 4 Liquid Chromatograph with an LC-95 UV/vis detector set at 260 nm. Atomic absorption spectroscopy was performed by using a Varian AA1475 instrument. X-ray diffraction data were collected on a Marresearch imaging plate system equipped with a Rigaku Cu rotating anode radiation source.

Deoxyoligonucleotide Synthesis and Purification. Deoxyoligonucleotides were prepared by using standard solid phase phosphoramidite methods. Protecting groups and excess trityl groups were removed by G25 Sephadex size exclusion chromatography, after which the deoxyoligonucleotides were lyophilized to dryness. Deoxyoligonucleotides were then converted to their sodium salts by using a Dowex cation exchange column.

The diaqua derivative of cisplatin was prepared by allowing 1.97 equiv of $AgNO_3$ to react with *cis*-[Pt(NH_3)$_2$$Cl_2$] in water at room temperature in the dark. After 12 h, the reaction mixture was centrifuged at 13 000 rpm for 10 min to remove AgCl. The aqueous layer was drawn away from the AgCl pellet by using a pipette and centrifuged for another 10 min. This process was repeated twice, and the final platinum solution was allowed to react with deoxyoligonucleotides containing a d(GpG) site at 37 °C in the dark for 6−8 h.

Platinated deoxyoligonucleotides and their complementary strands were initially purified by a 100−500 mM NaCl gradient on an ion exchange HPLC column and subsequently with a 5%−20% acetonitrile gradient on a C4 or C18 reverse phase HPLC column.

Crystallization. Purified complementary strands of each deoxyoligonucleotide were mixed in a 1:1 molar ratio and diluted to a concentration of 2.5 mM. Crystals were grown by using the sitting drop method. Each crystallization drop contained 0.2 mM duplex DNA, 52 mM cacodylic acid (sodium salt, pH 6.0), 15 mM $MgCl_2$, 6 mM [Co(NH_3)$_6$]Cl_3 and 3% 2-methyl-2,4-pentanediol (MPD). Crystallization drops were mixed at room temperature and equilibrated against a 5% MPD reservoir at 4 °C. Clusters of crystals with dimensions of about 0.05 × 0.10 × 1.0 mm appeared after 3−30 days and were allowed to grow for 9−12 months.

X-ray Data Collection. Crystals cut from clusters and measuring approximately 0.05 × 0.10 × 1.00 mm were mounted in glass capillaries containing a drop of mother liquor and sealed with melted wax. Data were collected on a Marresearch image plate with Cu Kα (λ = 1.5418 Å) radiation. Unit cell parameters were determined by autoindexing several images in each data set separately with the program DENZO (Z. Otwinowski, University of Texas, Southwestern Medical Center). From the cell constants and lack of systematic absences, the space group was chosen to be *P*1. For each data set, rotation images were collected in 3° increments with a total rotation of 360° about ϕ. Unit cell parameters, sequences used, and additional X-ray information are summarized in Table 1.

(13) Admiraal, G.; van der Veer, J. L.; de Graaff, R. A. G.; den Hartog, J. H. J.; Reedijk, J. *J. Am. Chem. Soc.* **1987**, *109*, 592.
(14) Sherman, S. E.; Gibson, D.; Wang, A. H.-J.; Lippard, S. J. *J. Am. Chem. Soc.* **1988**, *110*, 7368.
(15) Bellon, S. F., Ph. D. Dissertation, Massachusetts Institute of Technology, 1992.
(16) Takahara, P. M.; Rosenzweig, A. C.; Frederick, C. A.; Lippard, S. J. *Nature* **1995**, *377*, 649.
(17) Bellon, S. F.; Lippard, S. J. *Biophys. Chem.* **1990**, *35*, 179.
(18) Bellon, S. F.; Coleman, J. H.; Lippard, S. J. *Biochemistry* **1991**, *30*, 8026.
(19) Rice, J. A.; Crothers, D. M.; Pinto, A. L.; Lippard, S. J. *Proc. Natl. Acad. Sci. U.S.A.* **1988**, *85*, 4158.

Table 1. Experimental Details of the X−ray Diffraction Study of d(CCU^{Br}CTG*G*TCTCC)•d(GGAGACCAGAGG)

unit cell parameters	$a = 31.27$ Å $\alpha = 79.81°$ $b = 35.46$ Å $\beta = 84.75°$ $c = 47.01$ Å $\gamma = 82.79°$
unit cell volume	50 770 Å^3
space group	*P*1
molecules per asymmetric unit	2
instrument	Marresearch Imaging Plate
radiation	Cu Kα
diffraction limit	2.6 Å for Br1
structure solution method	multiple isomorphous replacement (MIR)
sequences used for MIR:	
native	d(CCTCTG*G*TCTCC)•d(GGAGACCAGAGG)
Br1	d(CCU^{Br}CTG*G*TCTCC)•d(GGAGACCAGAGG)
Br2	d(CCTCTG*G*U^{Br}CTCC)•d(GGAGACCAGAGG)
Br3	d(CCTCTG*G*TC^{Br}TCC)•d(GGAGACCAGAGG)

Data Collection, Reduction, and Structure Determination. Data were collected at 4 °C on a Marresearch imaging plate and processed by using DENZO, SCALEPACK (Z. Otwinowski), and the CCP4 program suite.[20] An anomalous difference Patterson map calculated from the native data revealed the relative positions of the platinum atoms and confirmed the presence of two platinated duplexes in each unit cell. The platinum atoms are 15.1 Å apart. Difference Patterson maps using the native and derivative data were calculated for each brominated duplex. These maps clearly showed one peak corresponding to a bromine−bromine vector, in accord with the presence of two DNA duplexes in the asymmetric unit.

The bromine positions were used to calculate single isomorphous replacement (SIR) phases for each heavy atom derivative. Fourier maps were then computed by using the SIR phases and the native structure factor amplitudes. From each SIR map, two pairs of possible platinum atomic positions were obtained. Shifting one platinum atom to the origin of the unit cell with concomitant shifting of the bromine atoms afforded two possible pairs of bromine positions for each derivative.

The various pairs gave eight possible combinations of heavy atom positions, each of which was used to calculate trial phases. The correct bromine coordinates for each derivative were found by choosing the best multiple isomorphous replacement (MIR) electron density map. Bromine positions were confirmed by calculating electron density maps with MIR phases and $||F_{nat}| - |F_{der}||$ structure factor amplitudes. The platinum atom positions were confirmed by calculating maps with MIR phases and the anomalous differences in the native data as the structure factor amplitudes.

An initial model of B-DNA modified with *cis*-$\{Pt(NH_3)_2\}^{2+}$ at the G6−G7 step was built with the program INSIGHT II (Biosym). Model manipulation was done by using the program O.[21] No symmetry restraints relating the two molecules in the unit cell were applied during refinement. The initial model was fit to the MIR maps calculated with native structure factor amplitudes to 3.0 Å. After positional refinement in X-PLOR,[22,23] the phases obtained were applied to the Br1 derivative data (Table 1) with $|F_{obs}|$ to 2.6 Å. A fraction (10%) of the reflections were set aside for the free-*R* factor calculation prior to model building and refinement.[24−26] Seventeen cycles of model building, positional refinement, and phase combination yielded a model for which $R = \sum(|(|F_{obs}| - |F_{calc}|)|/\sum|F_{obs}| = 0.25$. Another round of positional refinement in which all restraints on the platinum geometry were removed, followed by temperature factor refinement, resulted in $R = 0.225$. Finally, 31 water molecules were added to the model, giving a final structure with *R*-free = 0.249 and $R = 0.203$. The validity of this structure was checked by using a series of simulated annealing omit maps in which one base step at a time was omitted from the calculation. Refinement statistics are given in Table 2. The overall estimated coordinate error for this structure is 0.46 Å, determined by using a plot of $\ln(\sigma_A)$ vs resolution.[27,28]

Table 2. Crystallographic Information

crystal	resolution (Å)	no. of unique reflns	completeness (%)	R_{sym}[c] (%)	isomorphous difference (%)[d]	phasing power[e]
native	3.0	3793	97.7	6.2		
Br1	2.6	5797	97.0	6.2	13.4	1.4
Br2	3.0	3380	86.8	8.7	16.1	0.9
Br3	3.0	3488	89.9	7.5	17.1	0.9

R factor[a] = 0.203 *R*-free[b] = 0.245
rmsd: distances = 0.015 Å
angles = 3.1°
temperature factors = 1.9 Å^2

[a] R factor $= [\sum(hkl)||F_{obs}| - |F_{calc}||]/\sum(hkl)|F_{obs}|$. [b] *R*-free $= [\sum(hkl)||F_{obs}| - |F_{calc}||]/\sum(hkl)|F_{obs}|$ for reflections set aside before refinement. [c] $R_{sym} = [\sum(hkl)\sum(i)|I(hkl) - \overline{I(hkl)}|]/\sum(hkl)\sum(i)I(hkl)$. [d] Isomorphous difference $= R_{iso} = [\sum(hkl)||F_{deriv}| - |F_{nat}||]/\sum(hkl)|F_{nat}|$. [e] Phasing power $= [\sum|F_H|^2/\sum|E|^2]$ with $\sum|E|^2 = \sum[|F_{PH}|_{obs} - |F_{PH}|_{calc}]$.

Results

Unit Cell Composition and Crystal Packing. From the volume of the unit cell, 50 770 Å^3, and the approximate volume of a B-DNA base pair, 1700 Å^3, we estimated that there are two duplexes per unit cell.[29] This estimate was confirmed by the presence of one large peak in the anomalous difference Patterson map corresponding to a vector between two crystallographically independent platinum atoms.

Since molecular averaging was not used during the refinement, two independent determinations of the structure were obtained. We hereafter designate the two molecules as A and B. A ball-and-stick model of molecule A and the nucleotide numbering scheme are shown in Figure 1. Molecules A and B are related by a noncrystallographic rotation axis (Figure S1, Supporting Information) which does not extend to the neighboring unit cells (Figure S2). Molecules A and B have very similar structures even though they are not related by crystallographic symmetry. The root-mean-square deviation (rmsd) between all atoms is 0.38 Å, and an overlay of the two structures is available as Figure S3.

There are three types of duplex−duplex packing interactions in the crystal lattice: end-to-end, end-to-groove, and backbone-to-backbone. These combine to form an intricate network of DNA molecules containing large solvent channels (Figure 2). These channels have dimensions of 10−30 Å and reflect the high solvent content of the crystal. Computing the volume of the DNA from a mask generated in the program O and assuming

(20) Bailey, S. *Acta Crystallogr.* **1994**, *D50*, 760.
(21) Jones, T. A.; Bergdoll, M.; Kjeldgaard, M. In *Crystallographic Computing and Modeling Methods in Molecular Design*; Bugg, C., Ealick, S., Eds.; Springer-Verlag: New York, 1989.
(22) Brünger, A. T.; Kuriyan, J.; Karplus, M. *Science* **1987**, *235*, 458.
(23) Brünger, A. T. *X-PLOR Version 3.1. A System for X-ray Crystallography and NMR*; Yale University Press: New Haven, CT, 1992.
(24) Brünger, A. T. *Nature* **1992**, *355*, 472.
(25) Brünger, A. T. *Acta Crystallogr.* **1993**, *D49*, 24.
(26) Kleywegt, G. J.; Brünger, A. T. *Structure* **1996**, *4*, 897.
(27) Read, R. J. *Acta Crystallogr.* **1986**, *A42*, 140.
(28) Drenth, J. *Principles of Protein X-ray Crystallography*; Springer-Verlag: New York, 1994.
(29) Kennard, O.; Hunter, W. N. *Q. Rev. Biophys.* **1989**, *22*, 327.

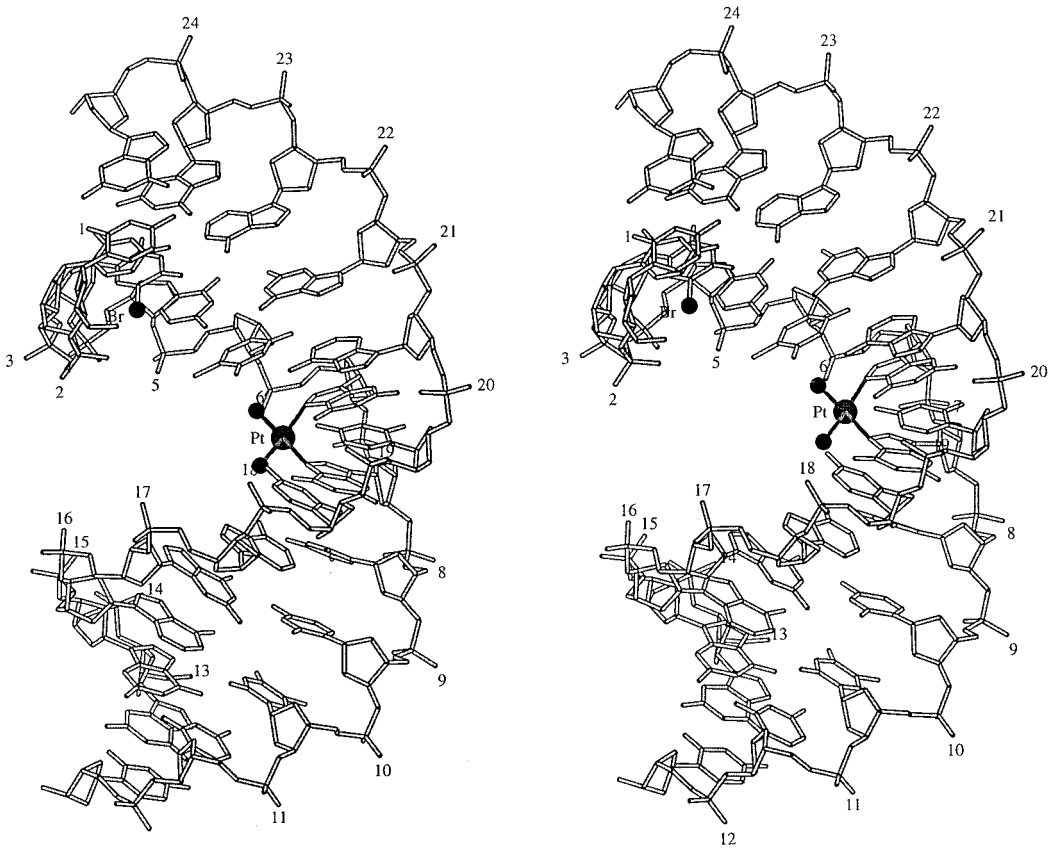

Figure 1. Stereoview of a ball and stick model of the duplex DNA, d(CCU^{Br}CTG*G*TCTCC)·d(GGAGACCAGAGG), where -G*G*- is modified by *cis*-{$Pt(NH_3)_2$}$^{2+}$.

that the rest of the unit cell to be filled with solvent, the solvent content was estimated to be ~60%.

The platinated DNA duplexes interact with one another through two types of hydrophobic packing contacts. In one such interaction, the 3′ end of one molecule, comprising base pair C12−G13, stacks against the 3′ end of another such that a pseudo-continuous helix forms. This type of packing is often observed in crystals of B-DNA.[30] The ends are held together by the hydrophobic stacking interaction of the terminal base pairs, with 3′ C12 base of one dodecamer stacking on the 5′ G13 of another. Along with directly stacking on the C12−G13 base pair of an adjacent duplex, the terminal base pair is also positioned in space directly above the C11−G14 base pair of the next helix. This interaction can be seen when the stacking is viewed down the helix axis (Figure S4). If the two stacked helices are considered to be a pseudo-continuous segment of B-DNA, then at the base step contact between the C12-G13 terminal base pairs of adjacent helices the DNA has a twist of −35° and unwinds a full step before resuming normal helical winding at the next base step. This unwinding is possible because the interaction between the terminal C12−G13 base pairs of adjacent helices is unconstrained by the sugar−phosphate linkage that would be present in a segment of continuous DNA.

In the second type of hydrophobic packing interaction, the 5′ terminal base pair, C1−G24, of each duplex abuts the minor groove of a neighboring helix (Figure 3), a feature often seen in crystals of A-DNA.[31,32] The end base pair of helix A packs against the hydrophobic surface of the sugar phosphate backbone on helix B (Figure S5a,b). The C1 base of helix A stacks over the deoxyribose C3′ atom of residue G7 on helix B, and G24 of helix A packs closely against the C1′ region of the deoxyribose ring of T8 on helix B. This interaction is hydrophobic in nature, although the overlap between the base and the ribose ring is less pronounced than the C1−G7 ribose interaction. A slightly different interaction takes place between the C1−G24 of helix B when it packs against the deoxyribose rings of G7 and T8 on helix A (Figure S5c,d). In this case, the purine ring of helix B G24 packs directly against the sugar of T8 on helix A. As in the case of helix A packing against the minor groove of helix B, C1 of helix B packs against the deoxyribose ring of G7, but to a lesser extent. These end-groove interactions are also stabilized by hydrogen bonds between the terminal C1−G24 base pair and the G6−C19 base pair of the helix, which accommodates its neighbor by opening and flattening its minor groove. The hydrogen bonding interactions, between N2 of G24 and O2 of C19 and between O2 of C1 and N2 of G6, and their distances are shown in Figure 4.

Molecules A and B also have close contacts between their backbones (Figure 5) which we ascribe to CH···O hydrogen bonding.[33,34] Such hydrogen bonds have been postulated to play an important role in the stabilization of unusual DNA strand interactions, such as A−T base pairs involving O2 of thymine and C2-H of adenine,[35a] and in close sugar-phosphate backbone packing which stabilizes cytosine-rich DNA quadruplexes.[35b] In the present structure, the participating atoms are a phosphate oxygen interacting with C4′-H and O3′ interacting with C5′-H. The backbone contacts between helices A and B are not related by pseudosymmetry. For example the T5 C4′-H atom of

(30) Wang, A. H.-J.; Teng, M.-K. *J. Cryst. Growth* **1987**, *90*, 295.

(31) Frederick, C. A.; Quigley, G. J.; Teng, M.-K.; Coll, M.; van der Marel, G.; van Boom, J.; Rich, A.; Wang, A. H.-J. *Eur. J. Biochem.* **1989**, *181*, 295.

(32) Wang, A. H.-J.; Fujii, S.; van Boom, J. H.; Rich, A. *Proc. Natl. Acad. Sci. U.S.A.* **1982**, *79*, 3968.

(33) Desiraju, G. R. *Acc. Chem. Res.* **1991**, *24*, 290.

(34) Derewenda, Z. S.; Lee, L.; Derewenda, U. *J. Mol. Biol.* **1995**, *252*, 248.

(35) (a) Leonard, G. A.; McAuley-Hecht, K.; Brown, T.; Hunter, W. N. *Acta Crystallogr.* **1995**, *D51*, 136. (b) Berger, I.; Egli, M.; Rich, A. *Proc. Natl. Acad. Sci. U.S.A.* **1996**, *93*, 12116.

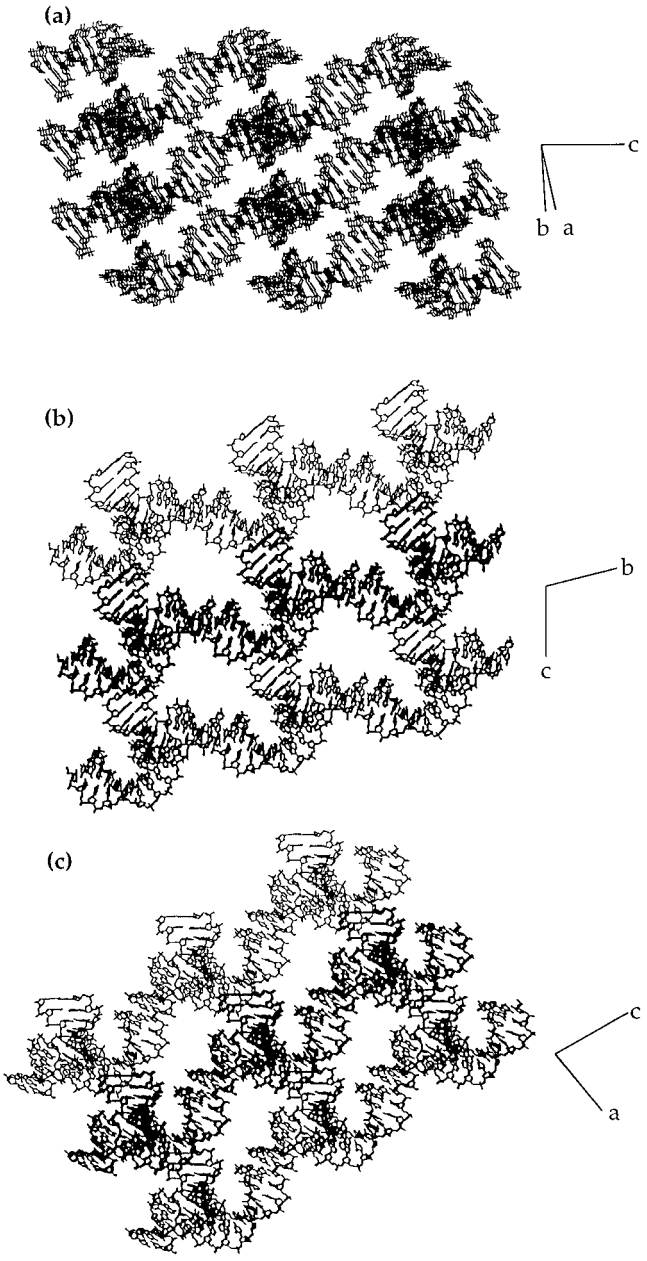

Figure 2. Packing diagrams showing the large solvent channels which run through the crystal of cisplatin-modified DNA.

molecule A forms a CH···O hydrogen bond with a G6 OP of molecule B whereas the T5 C4′-H atom of molecule B interacts with the T5 OP atom of molecule A. Although the stacking of the 3′ ends of neighboring helices appears to be identical for molecules A and B, the backbones and end-groove packing clearly reveal that the contacts between the two molecules differ. This result further underscores the slightly different packing environments and crystallographic independence of the two duplexes in the unit cell.

The solvent content of DNA crystals is generally high and often disordered, limiting the resolution.[28] Some ordered solvent molecules are usually seen for crystals which diffract to 2.6 Å resolution, and 31 water molecules were located in the present structure determination. The central four base pairs at the platination site of both molecules contain a high proportion of the ordered water molecules. Ten out of 18 waters associated with molecule A and 7 out of 13 waters associated with molecule B contact base pairs T5−A20 through T8−A17. The water molecules that were located are listed in Table S1 (Supporting Information), and their positions are shown schematically in Figure 6.

The Platinated DNA Duplex. The structures of the two crystallographically independent cisplatin-modified DNA duplexes are superimposed in Figure S3. The two molecules have the same general features. The 5′ end of each helix is A-like and the 3′ end is B-like, judging by nearest-neighbor phosphate−phosphate contacts, backbone torsion angles, and base step stacking patterns. This heterogeneity is especially clear when the helix is viewed down either end and compared to similar views of A-DNA and B-DNA (Figure S6).[16] The entire minor groove of each duplex, however, is quite wide and bears a general resemblance to A-DNA. We ascribe the origin of these features to distortion of the double helix at the site of platinum coordination. Small but significant differences between the two crystallographically independent molecules are revealed by evaluation of detailed structural parameters.

Helical base−base and base−step parameters used to describe the details of nucleic acid structures are defined according to the EMBO Workshop on DNA Curvature and Bending.[36] We present such parameters for the cisplatin-modified duplex and compare them to those of canonical A- and B-DNA in Tables 3 and 4 and Figures S7 and S8.

In electron density maps of a crystal structure at 2.6 Å resolution, individual atoms in the backbone cannot be resolved and many aspects of the structure must therefore be inferred from distances between phosphate groups. The distances between phosphorus atoms along the backbone and across the grooves are known quite precisely for the two independent molecules in the present structure. These values are the same within experimental error and are shown schematically in Figure S9. Groove widths and backbone distances are shown graphically in Figure S10; the major groove is less well determined because there are fewer distances with which to characterize it.

Structure of Molecule A. The first four base steps of helix A comprise base pairs C1−G24 through T5−A18 (Figure 1). This segment of the helix has an overall resemblance to canonical A-DNA. The A-like classification is based on deoxyribose ring conformations and the twist at each base step. All sugar puckers are either C3′-endo or C4′-exo, a conformation very close to that of A-DNA. At 2.6 Å resolution, the conformations of the sugar rings cannot be seen in electron density maps but must be inferred from distances between adjacent phosphate groups. The phosphate−phosphate distance is about 5.6 Å for a C3′-endo (A-DNA) sugar pucker and 6.5 Å for a C2-endo (B-DNA) sugar pucker. Phosphate distances along the double helix backbone are shown schematically in Figure S9 and graphically in Figure S10. Base pair parameters and base step parameters are presented in Figures S7 and S8, respectively, and backbone torsion angles are listed in Table 5.

Base step stacking interactions are another feature of DNA which can be used to classify the double helix as A-form or B-form. The base step stacking interactions for helix A are presented in parts a and b of Figures S11−S21. The stacking of the first two base steps (Figures S11 and S12) resembles typical A-DNA stacking; purine−purine sequences have the five-membered ring of one purine positioned over the six-membered ring of the next. Base steps 3 and 4 (Figures S13 and S14) are A-like in terms of their ring conformations and fall between A-DNA and B-DNA in their stacking interactions. In comparison to base steps 1 and 2, base steps 3 and 4 have slightly more pyrimidine ring overlap and less overlap between the five-membered ring of one purine base and the six-membered ring of the next in the sequence.

The fifth base step (Figure S15), which occurs between base pairs T5−A20 and G6−C19, is distorted because the N7 atom of G6 is coordinated to the platinum atom. Platinum coordina-

(36) Dickerson, R. E. *J. Biomol. Struct. Dyn.* **1989**, *6*, 627.

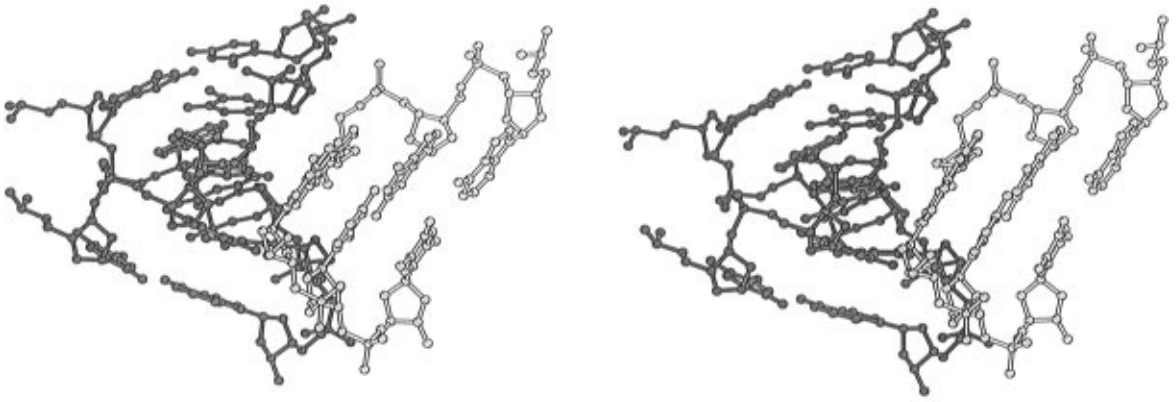

Figure 3. Stereoview of the end-to-groove packing interactions. The end of molecule A (light) is packing into the minor groove of molecule B (dark).

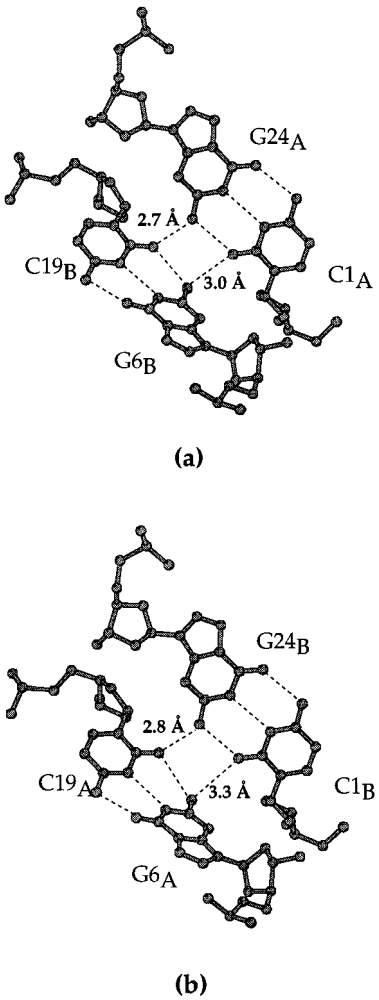

Figure 4. (a) Hydrogen bonding interactions between the C1−G24 base pair of molecule A and the G6−C19 base pair of molecule B. (b) Hydrogen bonding interactions between the C1−G24 base pair of molecule B and the G6−C19 base pair of molecule A.

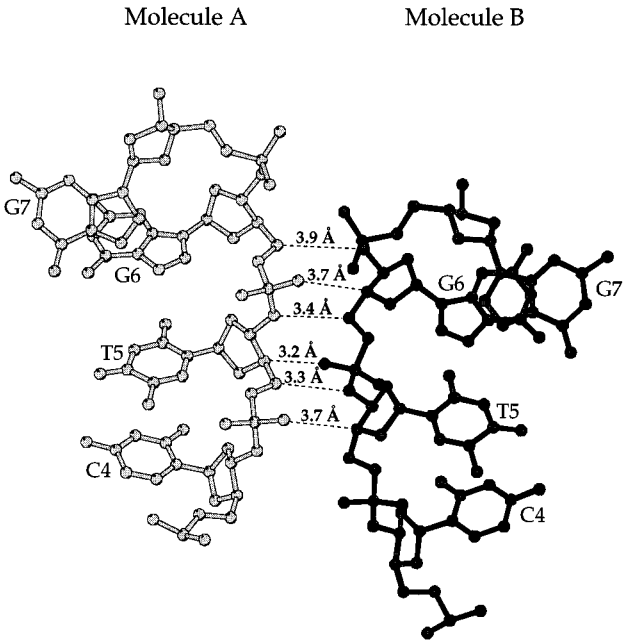

Figure 5. Backbone-to-backbone packing interaction between molecule A and molecule B. The interactions are between $T5_B$ C4′ (donor) and $T5_A$ O1P (acceptor, 3.7 Å), $T5_A$ C5′ (donor) and $T5_B$ O3′ (acceptor, 3.3 Å), $T5_A$ C4′ (donor) and $G6_B$ O1P (acceptor, 3.4 Å), $G6_B$ C5′ (donor) and $T5_A$ O3′ (acceptor, 3.2 Å), $G6_B$ C4′ (donor) and $G6_A$ O1P (acceptor, 3.7 Å), and $G6_A$ C5′ (donor) and $G65_B$ O3′ (acceptor, 3.9 Å).

tion causes a −1.7 Å shift at this base step and moves base pair G6−C19 toward the major groove. The shift positions A20 to span base pair G6−C19, which has a +13° buckle. The position of A20 and the nonplanarity of base pair G6−C19 allows stacking to be maintained between base pairs five and six despite the platinum lesion. Residue T5 of base pair five is pushed out into the major groove and does not participate in stacking with base pair G6−C19, but stacking of T5 with base pair C4−G21 and Watson−Crick hydrogen bonding between T5 and A20 are still maintained. The negative shift at this step is also stabilized by hydrogen bonding and end-groove packing interactions between G6−C19 and C1−G24 of a neighboring molecule, as discussed previously.

The sixth base step (Figure S16) occurs between base pairs G6−C19 and G7−C18 and both guanine residues have are bound to platinum at their N7 atoms. The coordination of platinum causes a roll of 26° toward the major groove with a concomitant opening of the minor groove. The roll at this base step is the main reason for the overall bend in the structure and probably facilitates the fusion of A-like and B-like segments of DNA. Platinum coordination also causes a positive shift at the sixth base step. Base pair G7−C18 is forced toward the minor groove as base pair G6−C19 is pulled toward the major groove in order to accommodate platinum binding. The five-membered ring of G7 stacks under the six-membered ring of G6, a situation which is the reverse of A-type stacking where the five-membered ring of the 5′ purine stacks over the six-membered ring of the 3′ purine. The cytosine residues which are paired with G6 and G7, C19 and C18, respectively, do not stack on one another but maintain base pairing while accommodating the guanine−guanine unstacking at the platinum

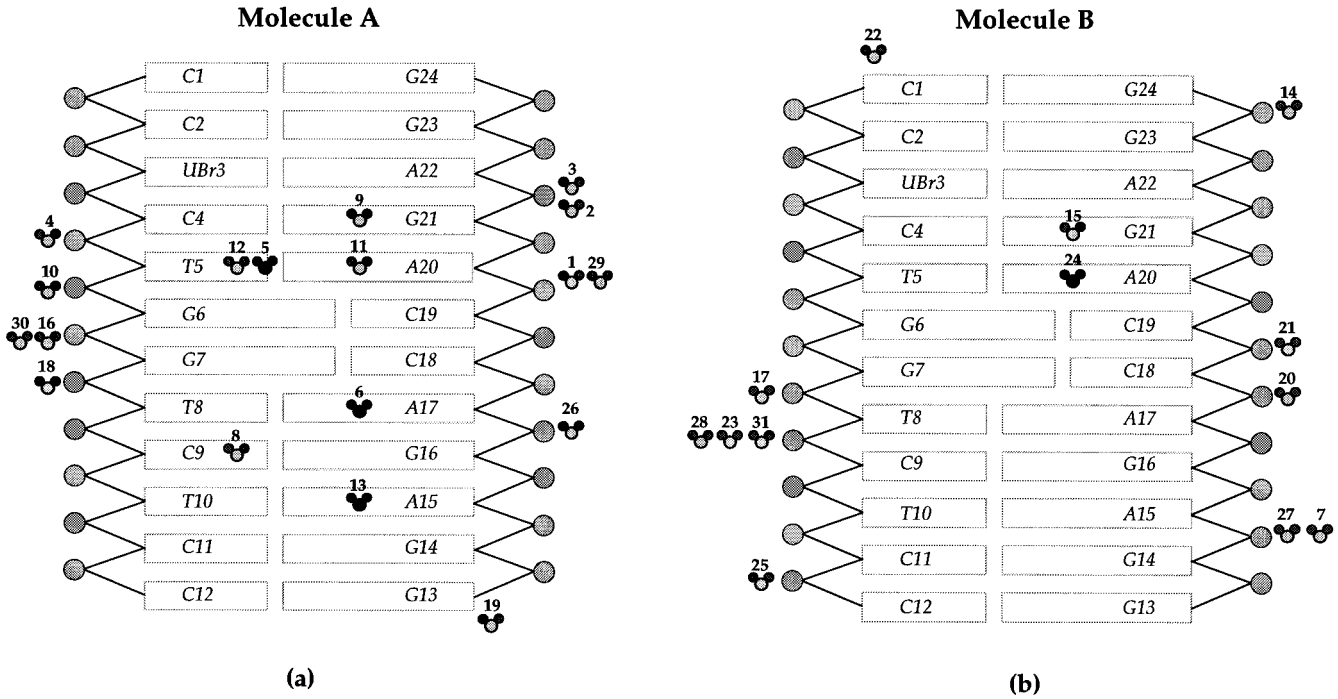

Figure 6. Schematic diagram of the water positions for (a) molecule A and (b) molecule B. The water molecules in the major groove are darkly shaded, and the water molecules along the backbone or in the minor groove are lightly shaded. Specific atom contacts and distances which range from 2.6 to 3.2 Å are listed in Table S1.

Table 3. Base Pair Parameters for Molecules A and B[a]

	κ		*σ*		*ω*		*Sx*		*Sy*		*Sz*	
	A	*B*	*A*	*B*	*A*	*B*	*A*	*B*	*A*	*B*	*A*	*B*
C1−G24	5.98	8.61	−3.76	−1.01	−5.96	−2.83	0.43	0.51	−0.47	−0.30	−0.25	−0.51
C2−G23	3.86	−2.48	−1.31	0.59	−5.40	−8.15	0.00	0.24	−0.33	−0.16	−0.12	−0.04
U(Br)3−A22	4.56	4.32	−1.65	1.48	−8.78	−9.94	−0.53	−0.48	−0.44	−0.16	−0.12	−0.31
C4−G21	−1.42	−1.76	6.24	5.73	−11.22	−10.02	0.42	−0.10	0.09	0.27	0.04	−0.05
T5−A20	4.66	6.01	8.60	2.65	−7.29	−8.90	0.91	0.42	0.11	−0.05	−0.05	0.01
G6−C19	13.07	12.96	−2.57	−1.49	−22.41	−15.66	0.47	−0.11	−0.23	−0.40	0.07	0.16
G7−C18	0.52	−1.46	2.00	4.74	−13.52	−18.67	−0.61	−0.29	−0.20	−0.01	0.26	0.15
T8−A17	9.92	−5.00	27.71	7.82	−40.49	−33.27	2.39	0.49	0.80	0.69	−0.51	0.20
C9−G16	−15.54	−14.16	10.21	3.48	−14.70	−12.31	−0.92	−0.09	0.20	−0.07	0.44	0.14
T10−A15	0.01	5.87	10.13	8.59	−8.34	−15.90	−0.36	0.39	0.17	0.76	0.03	−0.50
C11−G14	4.78	2.77	−3.95	−0.52	−13.48	−8.13	0.39	0.51	−0.33	−0.14	−0.54	−0.12
C12−G13	−0.53	−2.39	−1.69	1.49	1.31	−3.97	0.40	0.37	−0.22	−0.01	−0.31	−0.53
A-DNA	0.00	0.00	−0.85	−0.85	11.44	11.44	0.00	0.00	−0.11	−0.11	0.15	0.15
B-DNA	0.00	0.00	−0.38	−0.38	−1.29	−1.29	0.00	0.00	0.01	0.01	−0.02	−0.02

[a] Base pair parameters are defined as follows: *κ*, buckle; *σ*, opening; *ω*, propeller twist; *Sx*, shear; *Sy*, stretch; *Sz*, stagger.

Table 4. Base Step Parameters for Molecules A and B[a]

	ϱ		*τ*		Ω		*Dx*		*Dy*		*Dz*	
	A	*B*	*A*	*B*	*A*	*B*	*A*	*B*	*A*	*B*	*A*	*B*
C1−G24/C2−G23	−0.62	2.57	−4.69	−4.38	25.80	26.13	−0.54	−0.65	−2.42	−2.37	3.58	3.75
C2−G23/U(Br)3−A22	6.08	6.80	−0.60	1.38	29.55	29.22	−0.47	−0.45	−2.44	−2.34	3.38	3.22
U(Br)3−A22/C4−G21	6.14	7.14	−0.26	−0.87	36.14	29.80	0.75	0.63	−1.97	−1.97	3.63	3.58
C4−G21/T5−A20	2.08	3.60	1.78	−0.20	30.89	34.51	0.18	−0.02	−1.81	−1.79	3.26	3.25
T5−A20/G6−C19	12.21	5.63	−2.45	−3.00	27.57	24.62	−1.67	−1.08	−1.56	−1.81	3.26	3.40
G6−C19/G7−C18	25.17	26.94	1.30	3.69	24.22	29.98	1.37	1.66	−2.35	−2.34	3.69	3.63
G7−C18/T8−A17	0.66	4.06	9.33	2.89	51.29	39.10	0.61	−0.41	−0.24	−1.45	3.45	3.43
T8−A17/C9−G16	3.08	−0.66	−1.41	4.57	23.45	34.69	−0.86	0.49	−0.85	−0.94	3.76	3.53
C9−G16/T10−A15	8.33	11.66	3.76	9.18	29.93	30.96	−0.01	−0.10	−0.33	−0.13	3.02	2.97
T10−A15/C11−G14	7.44	4.81	3.45	−3.88	39.54	35.40	−0.26	−0.27	−0.51	−0.50	3.16	3.46
C11−G14/C12−G13	4.08	5.28	1.63	6.05	34.71	36.73	0.26	0.44	−0.67	−0.55	3.57	3.38
A-DNA	10.78	10.78	0.00	0.00	30.95	30.95	0.00	0.00	−2.08	−2.08	3.18	3.18
B-DNA	−2.80	−2.80	0.00	0.00	35.88	35.88	0.00	0.00	−0.62	−0.62	3.34	3.34

[a] Base step parameters are defined as follows: *ϱ*, roll; *τ*, tilt; Ω, twist; *Dx*, shift; *Dy*, slide; *Dz*, rise.

binding site. At this base step, there is also a change from negative slide to a slide of about zero, which demarcates the junction between A-like DNA and B-like DNA.

The seventh base step (Figure S17) comprises base pairs G7−C18 and T8−A17 and is the locus where most of the disruption caused by platinum binding occurs. Watson−Crick hydrogen bonding interaction within base pair T8−A17 is diminished but not totally abolished (Figure 7). The N6 atom of A17 is hydrogen bonded to O6 of G7 rather than to O4 of T8, but N1 of A17 remains hydrogen bonded to N3 of T8. The unusual

Table 5. Pseudorotation Angles, Sugar Puckers, and Torsion Angles for Molecules A and B[a]

base	*P*	pucker	α	*β*	*γ*	*δ*	*ϵ*	*ζ*	*χ*
				Molecule A					
CYT 1	31	C3′−endo	−71	172		85	−164	−73	−164
CYT 2	20	C3′−endo	−85	179	59	84	−161	−67	−168
UBR 3	24	C3′−endo	−73	174	55	76	−168	−63	−161
CYT 4	19	C3′−endo	−62	162	61	83	−153	−77	−163
THY 5	15	C3′−endo	−69	−178	57	78	−169	−85	−155
GUA 6*	4	C3′−endo	−75	165	46	91	−149	−54	−144
GUA 7*	61	C4′−exo	−73	154	75	84	−164	−80	−167
THY 8	10	C3′−endo	−77	169	65	89	−165	−81	−135
CYT 9	26	C3′−endo	−66	177	64	90	−168	−68	−154
THY 10	162	C2′−endo	−68	178	65	136	−170	−94	−118
CYT 11	149	C2′−endo	−74	−179	55	134	−177	−97	−104
CYT 12	154	C2′−endo			59	144			−108
GUA 24	178	C2′−endo			−151	159			−164
GUA 23	27	C3′−endo	126	−107	55	79	−166	−116	−163
ADE 22	21	C3′−endo	−75	179	59	83	−156	−69	−165
GUA 21	18	C3′−endo	−80	179	66	81	−155	−68	−167
ADE 20	18	C3′−endo	−69	160	164	87	−155	−76	−165
CYT 19	24	C3′−endo	165	−178	59	83	−156	−64	−158
CYT 18	24	C3′−endo	−78	−174	56	82	−167	−78	−157
ADE 17	26	C3′−endo	−78	173	60	77	−167	−60	−156
GUA 16	152	C2′−endo	−79	138	52	145	−148	−146	−93
ADE 15	174	C2′−endo	−65	175	52	144	178	−95	−95
GUA 14	145	C2′−endo	−84	−142	55	135	174	−91	−122
GUA 13	168	C2′−endo	−66	165		146	−163	−110	−123
				Molecule B					
CYT 1	27	C3′−endo	−72	173		80	−171	−71	−163
CYT 2	19	C3′−endo	−87	−177	61	83	−159	−70	−171
UBR 3	24	C3′−endo	−74	171	61	80	−161	−61	−155
CYT 4	24	C3′−endo	−81	−177	62	80	−165	−68	−164
THY 5	20	C3′−endo	−71	174	56	81	−169	−77	−155
GUA 6*	13	C3′−endo	−79	161	59	85	−139	−51	−153
GUA 7*	47	C4′−exo	−77	162	75	75	−162	−80	−168
THY 8	19	C3′−endo	−72	172	67	91	−164	−67	−153
CYT 9	39	C4′−exo	−66	−178	61	88	−173	−71	−149
THY 10	179	C2′−endo	−70	−177	63	146	−180	−98	−98
CYT 11	154	C2′−endo	−72	−180	53	140	−171	−102	−105
CYT 12	164	C2′−endo			55	146			−103
GUA 24	162	C2′−endo			−170	151			−172
GUA 23	22	C3′−endo	146	−112	54	76	−177	−107	−161
ADE 22	20	C3′−endo	−76	171	59	83	−150	−67	−164
GUA 21	12	C3′−endo	−78	174	58	85	−163	−60	−159
ADE 20	23	C3′−endo	−67	168	175	80	−151	−77	−173
CYT 19	26	C3′−endo	143	−153	54	81	−157	−76	−163
CYT 18	17	C3′−endo	−91	−170	64	89	−156	−76	−164
ADE 17	14	C3′−endo	−72	170	56	84	−152	−69	−157
GUA 16	146	C2′−endo	−70	137	53	145	−158	−158	−97
ADE 15	155	C2′−endo	−78	176	57	138	−167	−94	−110
GUA 14	159	C2′−endo	−71	−179	50	143	−170	−104	−117
GUA 13	166	C2′−endo	−71	176		142	−167	−121	−103

[a] Torsion angles are defined as Phos−α−O5′−*β*−C5′−*γ*−C4′−*δ*−C3′−*ϵ*−O3′−*ζ*−Phos. *χ* is the glycosyl torsion angle, and *P* is the pseudorotation angle.

hydrogen bonding is apparent from the positive shear, stretch, opening, and buckle and by the negative stagger and −33° to −40° propeller twist within this base pair (Tables 3 and 4). The distortion is compensated for by a highly twisted stacking interaction between T8−A17 and G7−C18. In base step seven, G7 is stacked directly on top of T8 whereas C18 sits directly over A17. This type of stacking is unusual, does not resemble features in either A- or B-DNA, and is the origin of the large positive twist and the positive tilt at this step. Further compensation for the large helical disruption at the seventh base step comes from a negative buckle at base pair C9−G16 and a negative stagger at base pair C11−G14, both of which keep the bases of the double helix stacked in an energetically favorable manner.

The negative buckle at C9−G16 and the negative stagger at C11−G14 are minor local base pair adjustments and do not affect the overall helical structure of the last four base steps on helix A. Steps eight through eleven (Figures S18−S21) which include base pairs T8−A17 to C12−G13, are fairly uniform in structure, and more closely resemble B-DNA. This similarity is best appreciated by the distances between adjacent phosphates on both the platinated and unplatinated strands, all of which are closer to the 6.5 Å value of B-DNA than the 5.6 Å value of A-DNA.[37] Furthermore, the base stacking pattern of each step is very similar to that in B-DNA.

Structure of Molecule B. As previously stated, helix B has the same overall shape as helix A. The sugar puckers and base stacking patterns are the same as for helix A and show a transition from A-like DNA on the 5′ side of the platinum lesion to B-like DNA on the 3′ side. The base pair and base step parameters are the same for helices A and B from the first base pair, C1−G24, to the seventh, G7−C18 (Figures S11−S17). Differences between the two independent molecules are subtle and become most evident at base step seven (Figure S17),

(37) Saenger, W. *Principles of Nucleic Acid Structure*; Springer-Verlag: New York, 1984.

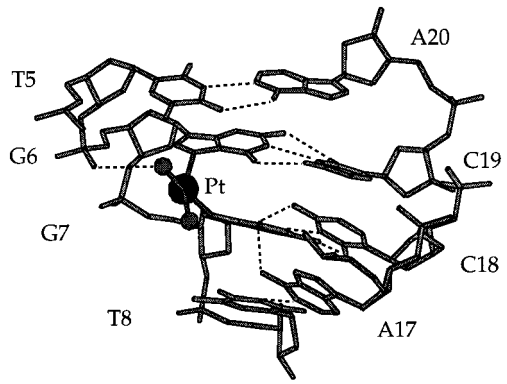

Figure 7. -G*G*- platination site. The base pairs are propeller twisted but retain their hydrogen bonds. One of the ammine ligands on platinum is hydrogen bonded to a phosphate group on the backbone of the platinated deoxyoligonucleotide strand.

between G7−C18 and T8−A17. For molecule B, all base steps are shown in Figures S11−S21, sections c and d.

In helix A, disruption at the seventh base step comprises a positive twist and positive tilt, but these parameters are more normal in helix B. The base pair parameters at this step also differ slightly. Helix B has only positive stretch and negative propeller twist at base pair eight, T8−A17, and does not have unusual shear, opening, stagger or buckle observed in pair eight in helix A (Tables 3 and 4). Atom N6 of A17 is hydrogen bonded to O6 of G7 in helices A and B, but the complementary base, T8, is propeller twisted differently in helices A and B. Loss of a hydrogen bond within the T8−A17 base pair makes it much more flexible than the other base pairs and is presumably the reason why it adopts different orientations in the two independent molecules.

In molecule B the positive tilt occurs farther down the helix, at base step nine (Figure S19), between C9−G16 and T10−A15. Several base pair parameters are also subtly different in this region. Base pair nine has negative buckle in both helices, but base pair ten, which appears normal in helix A, has a positive stretch and a negative stagger in helix B. Helix B also has a negative stagger farther down the helix at base pair twelve instead of at base pair eleven as was seen in helix A. These base pairs and their stacking interactions are shown in Figures S20−S21.

The base pair disruptions in molecules A and B differ, but the overall shape of the two independent helices remains generally the same and the molecules can easily be superimposed on one another, as indicated in Figure S3. The overall shape is approximately the same within experimental error for molecules A and B and is mainly the result of a significant bend in the DNA, discussed next.

Bending. Helix axes for molecules A and B as calculated with the program CURVES[38,39] are depicted in Figure 8 viewed perpendicular to the plane formed by the platinum atom and its two ammine ligands. The bend for each molecule was measured manually in this orientation. For reference, the solution structure of a cisplatin-modified duplex octamer with a reported bend of 58° is also shown in the figure.[40] Molecules A and B have slightly different bend angles and helical axes because they have slightly different parameters for the eighth through eleventh base steps. The overall bend for both helices appears to be ∼35−40° and is distributed over several base pairs around the site of platinum coordination, with the major component arising from the +26° roll between the platinated guanosines. A more exact bend angle can be calculated for each helix by using the helix axis of the three terminal base pairs of the B-type segment and the helix axis of the five terminal base pairs of the A-DNA segment. One axis is translated such that its endpoint superimposes onto that of the other axis and, in this orientation, a 39° bend is obtained for helix A and a 55° bend is calculated for helix B. The bend angle calculated in this manner from coordinates of the NMR solution structure is 34°, considerably less than the reported value of 58°. The difference between the bends for molecules A and B in the crystal structure reflects the lack of a point of intersection for the axes and our inability to determine an exact helix axis with only three base pairs in the B-type fragment. Although this analysis reveals the difficulty in calculating rigorously the bend angles of the platinated duplex, Figure 8 nonetheless reveals that the intrastrand *cis*-$\{Pt(NH_3)_2\}^{2+}$ cross-link substantially alters the direction of the helix axis.

Details of the Platinum Binding Site. A view of the metal binding interaction (Figure 7) illustrates the large positive roll caused by coordination of platinum to the N7 atoms of adjacent guanosine residues. The dihedral angle between the two guanine rings is approximately 26°, far less than the ∼80° angle found in the crystal structure of *cis*-[$Pt(NH_3)_2${d(pGpG)}].[14] As observed in the latter structure, one of the ammines in the present structure is within hydrogen bonding distance of a phosphate oxygen atom, the $NH_3\cdots O$ distance being 3.3 Å for molecule A and 3.7 Å for molecule B.

The platinum atom is coordinated to N7 of G6 and to N7 of G7 and all platinum−nitrogen distances are about 2.0 ± 0.1 Å. The $\{Pt(NH_3)_2\}^{2+}$ moiety, the individual platinum atom and NH_3 groups of which are not resolved at 2.6 Å resolution, and the guanine bases have very well defined positions and the final model nicely fits the electron density (Figure 9). All four platinum−nitrogen bonds were left unrestrained during the final stages of refinement and converged to the expected distances of 2.0 Å. The platinum atom is not perfectly square-planar, but the deviations from normal angles and planarity are not significant at the present resolution. In both molecules A and B, the displacement of the metal atom from the planes of the G6 and G7 rings, by 1.2 and 0.8 Å, respectively, is highly significant, however, and clearly revealed by the electron density maps. The platinum centers have the same structures in molecules A and B, with an rmsd for all atoms in base pairs six and seven being 0.10 Å.

Discussion

Crystal Structure of Cisplatin-Modified DNA. The crystal structure described here is the first X-ray determination of a segment of duplex DNA containing the major adduct of the anticancer drug cisplatin. The data reveal that, when *cis*-$\{Pt(NH_3)_2\}^{2+}$ binds to adjacent guanosine residues on duplex DNA, it severely distorts the double helix by causing a bend toward the major groove and a widening and flattening of the minor groove. The shape of the cisplatin-modified DNA double helix probably accounts for the difficulty in crystallizing it. The structure of the double helix modified by cisplatin contains a junction of A-like and B-like DNA segments and is accommodated in the crystal lattice by a combination of A-DNA and B-DNA type packing motifs.

The crystals used in this study afford two crystallographically independent views of the structure. Two slightly different ways in which a segment of duplex DNA can accommodate a *cis*-$\{Pt(NH_3)_2\}^{2+}$ lesion are manifest. Despite these minor differences the two molecules have nearly identical global features indicating that the structure obtained is probably not just an artifact of crystal packing forces.

(38) Lavery, R.; Sklenar, H. *J. Biomol. Struct. Dyn.* **1988**, *6*, 63.
(39) Lavery, R.; Sklenar, H. *J. Biomol. Struct. Dyn.* **1989**, *6*, 655.
(40) Yang, D.; van Boom, S. S. G. E.; Reedijk, J.; van Boom, J. H.; Wang, A. H.-J. *Biochemistry* **1995**, *34*, 12912.

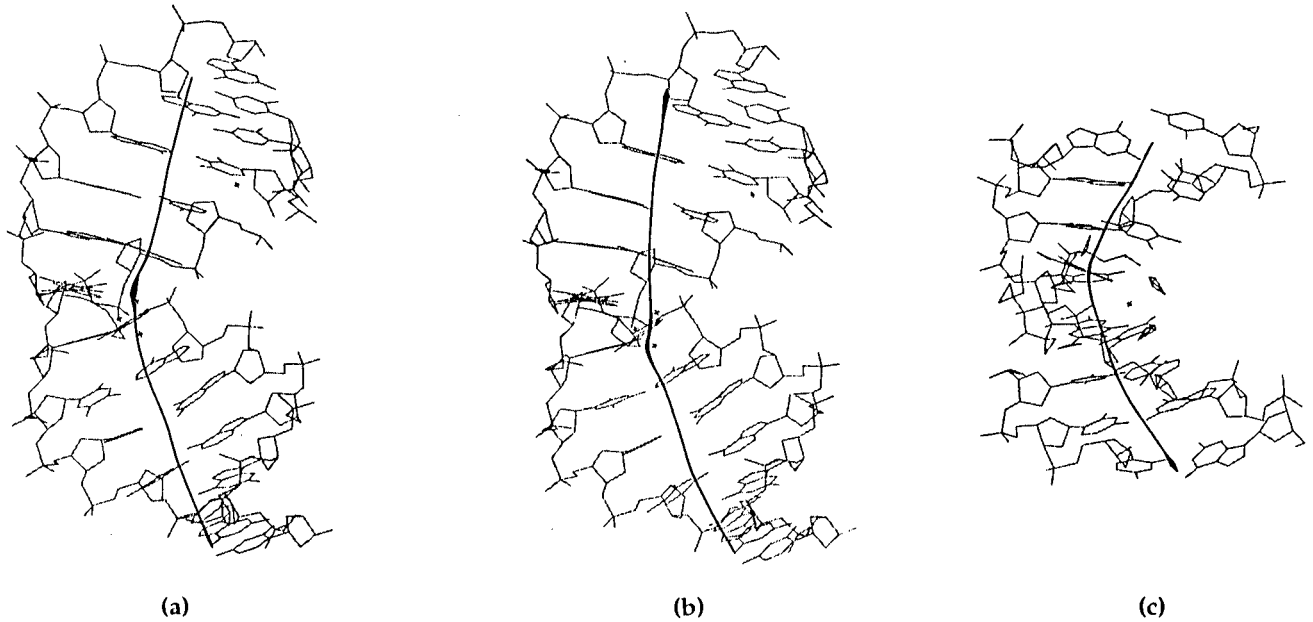

Figure 8. Helical axes calculated with the program CURVES for (a) molecule A, (b) molecule B, and (c) the NMR solution structure.

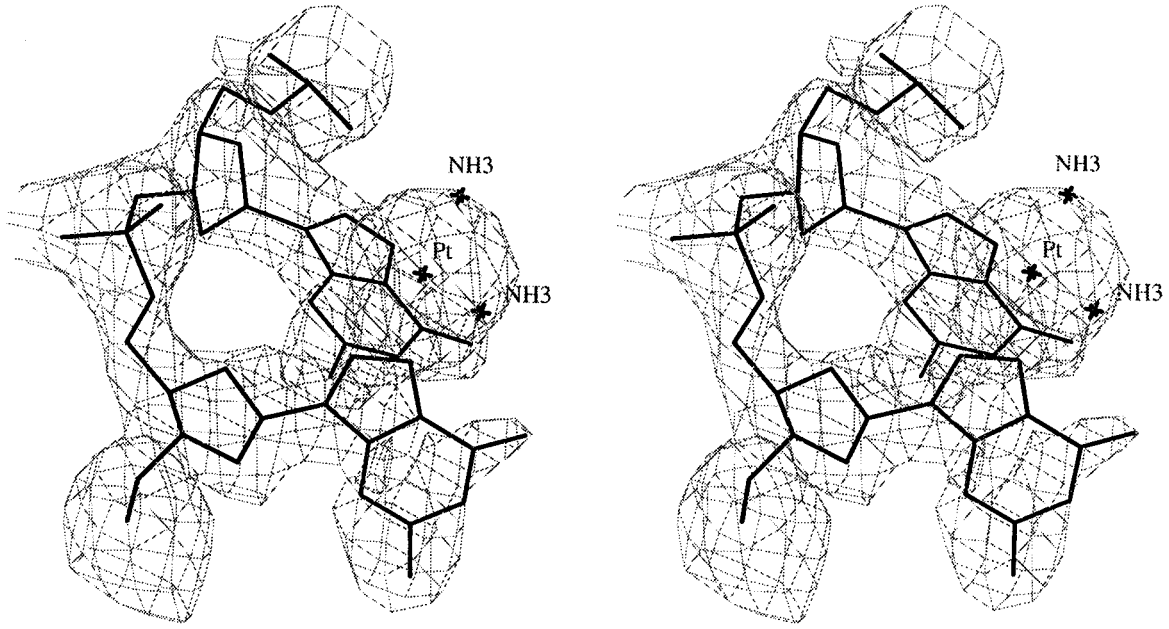

Figure 9. Stereoimage of *cis*-$\{Pt(NH_3)_2\}^{2+}$ bound to a d(GpG) site on duplex DNA. The $2F_o - F_c$ electron density map is shown in light gray and is contoured at 1σ. The platinum atom is shown coordinated to two ammines and the N7 atoms of adjacent guanine rings.

When *cis*-$\{Pt(NH_3)_2\}^{2+}$ forms an intrastrand cross-link between adjacent guanine residues on duplex DNA, it causes a large positive roll between the base pairs. This roll compresses the major groove while concomitantly opening up the minor groove and causing a bend which spreads out over the adjacent base pairs. The overall structure of the double helix remains intact and most of the distortion is absorbed by conformational changes in the sugar-phosphate backbone and base pair parameters for those residues near the platinum lesion. The DNA backbone is relatively flexible and its torsion angles are correlated so as to allow local fluctuations in the structure of a segment of DNA while maintaining the overall geometry of the double helix.[41] In the case of cisplatin-modified DNA, the phosphate groups on the backbone move closer together at the site of platinum binding. In addition, the backbone on the complementary strand adopts *t,t* rather than g^-,g^+ α and γ angles (Table 5) between nucleotides C19 and A20. These alterations better accommodate the positive charge and the widening of the minor groove. Compression of the phosphate backbone causes the sugar puckers of the residues to the 5′ side of the platinum lesion to adopt a C3′-endo conformation while the deoxyribose rings of the T10−C12 segment at the 3′ end of the helix remain in the C2′-endo conformation.

The A-type conformation to the 5′ side of the platinum lesion is propagated all the way to the 5′ end of the helix because the minor groove adopts a wide and flat conformation to accommodate the groove packing interaction of the C1−G24 base pair of a neighboring molecule. The 3′ end of the helix maintains a conformation closely resembling that of B-DNA. Previous work revealed that DNA having an A/B junction would display an overall bend of about 26°,[42] which happens to be the roll angle between the bases coordinated to *cis*-$\{Pt(NH_3)_2\}^{2+}$. Platination is most likely the cause of the structure observed, and the presence of A-like and B-like DNA conformations

(41) Kennard, O.; Salisbury, S. A. *J. Biol. Chem.* **1993**, *268*, 10701.

(42) Selsing, E.; Wells, R. D.; Alden, C. J.; Arnott, S. *J. Biol. Chem.* **1979**, *254*, 5417.

would appear to be stabilized by the crystallization conditions employed.

The complex $[Co(NH_3)_6]^{3+}$, used in place of spermine to stabilize the negative phosphate backbone during crystallization, is routinely added to DNA crystallization solutions. It facilitates conversion of B-form DNA to A-form DNA in solution[43,44] and stabilizes unusual DNA structures such as cruciforms.[45] The effect of $[Co(NH_3)_6]^{3+}$ on the crystal structure of cisplatin-modified DNA presented here cannot be evaluated because no electron density corresponding to a hexaamminecobalt(III) ion was located during the structure refinement, although the complex was necessary for crystal formation. The junction of A-like and B-like DNA seen in the platinated DNA structure proves that the conditions under which these crystals grow can support the coexistence of A- and B- DNA segments and that these conformations are probably quite similar in energy.[46]

A recently determined X-ray structure of an RNA−DNA hybrid reveals a similar coexistence of A-form and B-form DNA in a crystal. The structure of the duplex, (5′-uucgggcgcc-3′)• d(5′-GGCGCCCGAA-3′), is predominantly A-form, but the last three bases at the 3′ end of the DNA strand flip to B-form to facilitate stacking against a neighboring molecule and formation of a pseudo-continuous helix.[47]

The structure of cisplatin-modified DNA also reveals extended contacts between the backbones of the two crystallographically independent helices. These backbone interactions appear to be stabilized by CH···O hydrogen bonds. This type of hydrogen bonding has been observed in biologically significant structures[33] and has been suggested as a stabilizing interaction in non-Watson−Crick base pairs and four-stranded intercalated DNA.[35] The particular CH···O interactions we observe appear to be a feature unique to our structure, however. The series of hydrogen bonds between the backbones is probably critical for stabilization of the observed structure and crystal formation.

Comparison with a Recent NMR Solution Structure. Recently, an NMR solution structure of d(CCTG*G*TCC)• d(GGACCAGG), where G*G* denotes the *cis*-$\{Pt(NH_3)_2\}^{2+}$ coordination site, was reported.[40] This work confirmed the conversion of the 5′ platinated guanosine conformation from C2′-endo to C3′-endo found in numerous earlier NMR studies of the *cis*-$\{Pt(NH_3)_2\}^{2+}$ 1,2-intrastrand d(GpG) cross-link.[11] The bend angle was 58°, in agreement with molecular mechanics studies,[48] but considerably larger than the 32°−40° angle estimated by gel electrophoresis experiments[17,19] and the present 2.6 Å crystal structure.[16] Analysis of the bend from the published coordinates as described above, however, gave a more consistent value of 34°. The NMR solution structure has many features in common with the present crystal structure determination, including a similar dihedral angle of 23° between guanine rings coordinated to platinum, minimal disruption of base pairing at the platination site, and a wide, flat minor groove opposite the site of platinum coordination.

There are some significant differences between the solution and crystal structures. The probable hydrogen bond observed between one of the ammine ligands on platinum and a phosphate oxygen in the crystal structure was not observed in the solution structure, possibly due to the different buffer and salt environments used for the X-ray and NMR experiments. In the solution structure, the sugar ring on the 5′ side of the platinum lesion adopts the C3′-endo conformation, but the ring puckers for the rest of the double helix are similar to those of B-DNA; the crystal structure shows a combination of A-like and B-like helices. Because the structures are so different with respect to helical types, the bend angles cannot be precisely compared. It is obvious, however, that platinum binding severely distorts and bends duplex DNA toward the major groove, and that the magnitude of the bend is in general agreement with the results of gel electrophoresis bending studies of the platinated DNA.[17,19]

Structural information obtained from solution NMR and X-ray crystallographic studies of cisplatin-modified DNA complement each other and together provide a detailed picture of the distortions caused by platinum coordination. NMR measurements can afford very precise information about short-range distances, especially base pairing patterns and deoxyribose ring conformations. Limitations in the method make it difficult to determine long-range distances and a reliable model for groove shapes. This problem may be overcome by the use of paramagnetic spin labels to obtain long-range distance constraints in NMR structure determinations of short single-stranded[49] and larger duplex[50] DNA molecules. X-ray crystallography, on the other hand, is limited by crystal quality which controls the resolution of the diffraction data collected. At the 2.6 Å resolution of the structure reported here, electron density maps do not reveal the sugar puckers. The maps do, however, clearly show the positions of phosphorus and platinum atoms as well as the planes of the bases. From the phosphate−phosphate distances along the backbone, sugar pucker can be determined and groove widths measured. Packing interactions in crystals may influence the structure observed. The latter concern, however, is partially obviated by the extremely high solvent content (∼60%) of the crystals used in this investigation, which corresponds to a DNA concentration of 65 mM. The packing interactions we observe reveal interesting contacts between neighboring nucleic acid helices and may indicate how DNA−DNA or protein−DNA contacts involving platinated nucleic acids might occur in vivo.

In both the solution and crystal structures of the d(GpG) intrastrand cross-link of *cis*-$\{Pt(NH_3)_2\}^{2+}$ on DNA, the bend occurs over several base pairs and the major component is a large positive roll between coordinated GC base pairs. The roll results in a wide minor groove with a large hydrophobic surface which might be a good target for protein binding. This hydrophobic groove was a key feature in the crystal packing, where the end base pair of one helix was able to lodge tightly in the minor groove of its neighbor.

The crystal structure also reveals a potential for drug design based on platinum coordination compounds. The major groove, which contains the platinum atoms, has many functional groups which might interact favorably with ligands other than simple ammines. Octahedral metal complexes are currently in clinical use as chemotherapeutic agents.[51] An octahedral metal fragment such as *cis*-$\{M(L)_4\}^{2+}$, where M is a metal such as ruthenium and L is a small ligand such as an ammine, fits into the structure and binds two guanine residues in place of *cis*-$\{Pt(NH_3)_2\}^{2+}$, the major groove is large enough to accommodate moieties larger than the *cis*-$\{Pt(NH_3)_2\}^{2+}$ fragment. A similar exercise with the dinucleotide structure, *cis*-[$Pt(NH_3)_2$\{d(pGpG)-N7(G_1),-N7(G_2)\}], showed some unacceptably close contacts between the ligands and the guanine rings.[14] These were not apparent in the cisplatin-duplex crystal structure owing to the smaller roll between guanine ring planes.

(43) Gao, Y.-G.; Robinson, H.; van Boom, J. H.; Wang, A. H.-J. *Biophys. J.* **1995**, *69*, 559.
(44) Robinson, H.; Wang, A. H.-J. *Nucleic Acids Res.* **1996**, *24*, 676.
(45) Duckett, D. R.; Murchie, A. I. H.; Lilley, D. M. J. *EMBO J.* **1990**, *9*, 583.
(46) Doucet, J.; Benoit, J.-P.; Cruse, W. B. T.; Prange, T.; Kennard, O. *Nature* **1989**, *337*, 190.
(47) Horton, N. C.; Finzel, B. C. Submitted for publication.
(48) Kozelka, J.; Chottard, J.-C. *Biophys. Chem.* **1990**, *35*, 165.
(49) Dunham, S. U.; Lippard, S. J. *J. Am. Chem. Soc.* **1995**, *117*, 10702.
(50) Dunham, S. U.; Lippard, S. J. Unpublished results.
(51) Esposito, G.; Cauci, S.; Fogolari, F.; Alessio, E.; Scocchi, M.; Quadrifoglio, F.; Viglino, P. *Biochemistry* **1992**, *31*, 7094.

Postulated Stabilization of the Cisplatin Lesion by Further Duplex Bending. In order to accommodate a shallow dihedral angle of ∼26° between the planes of G6 and G7, the platinum atom lies out of the guanine planes by ∼1 Å. This result differs significantly from that of the X-ray crystal structure of *cis*-$\{Pt(NH_3)_2\}^{2+}$ coordinated to d(pGpG), in which the corresponding dihedral angle is ∼80° and platinum deviates by no more than 0.4 Å from the purine ring planes. The model derived to account for the NMR data also did not show a large deviation of platinum from the planes of the coordinated guanines, but the structure refinement was based on the platinated d(GpG) crystal structure results and on constraints applied in earlier modeling studies, none of which allowed metal−N7 bond bendability.[40]

A modeling study of cisplatin bound to duplex DNA was previously carried out with data from the X-ray structure of cyclic diguanylic acid crystallized with $CoCl_2$.[52] In this structure, cobalt binds to the N7 atoms of adjacent guanine residues and results in a roll of 33° between the guanine base planes. These results were used to model cisplatin binding to a duplex decamer, d(CAATG*G*ATTG)·d(CAATCCATTG), with platinum at the G*G* site. The structure was minimized and the resulting duplex had an overall bend of ∼34°, much less than had been predicted by earlier molecular mechanics calculations but in agreement with gel electrophoresis studies.[17,19] The diminished bend in the cobalt-derived model and in the present crystal structure of cisplatin bound to duplex DNA reveal the ability of the latter to induce strain at the metal center and indicate that metal−N7 bonds have more flexibility than previously thought. This feature might play an important role in the anticancer activity of the drug, because protein binding can further bend platinated DNA and perhaps be energetically driven by release of strain at platinum arising from the 1,2-intrastrand cross-link.

The idea that proteins might bind to bent cisplatin/DNA lesions and further distort them to provide an energetically more favorable state suggests a dependence on local sequence context. Previous modeling studies indicated that the sequence d(TG*G*) would be favored over d(CG*G*) for cisplatin binding.[53] Although such a preference has not been proved, it is interesting to consider, especially if a protein were to bind the platinated DNA and further bend the double helix toward the major groove. In the present crystal structure of *cis*-$\{Pt(NH_3)_2\}^{2+}$ bound to duplex DNA, O4 of T5 is about 5.1 Å from N4 of C19, which is base paired to platinated residue G6 (Figure 10a). If the helix were more significantly bent, these atoms would move closer together and could be positioned for a hydrogen bonding interaction. If T5 were replaced by a cytosine, then position 4 of the pyrimidine ring would be occupied by an exocyclic amino group, and there would be a steric clash upon further bending of DNA following protein binding (Figure 10b). Such an interaction does not occur on the 3′ side of the platinum lesion. The sequence G*G*T would not be preferred over G*G*C because the cytosine complementary to the platinated guanine, C18, is pushed up and away from T8 so that it can maintain good stacking interactions with A17 and C19.

A consideration of the sequences GG*G* and AG*G* affords a similar conclusion. Replacement of T5 by guanosine would position an oxygen atom, O6, 5.1 Å from N4 of C19 which might form a hydrogen bond if the helix were more significantly bent (Figure 10c). An adenine substituted for T5 would place an exocyclic amine group, N6, in the major groove, which would cause a steric clash with N4 of C19 if the DNA were bent further (Figure 10d).

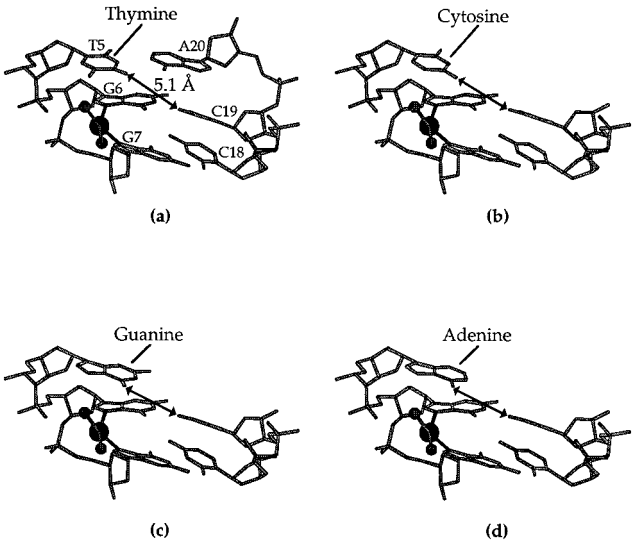

Figure 10. (a) TG*G* segment from the crystal structure of cisplatin-modified DNA. The O4 atom of residue T5 is 5.1 Å from the N4 atom of residue C19 in the current structure. Model with TG*G* replaced by (b) CG*G*, (c) AG*G*, and (d) GG*G*.

Coordination of ligands other than *cis*-ammine moieties to the platinum atom could also influence bending. In the case of a square-planar metal complex with an amino acid such as lysine[54] or a peptide in place of *cis*-ammine ligands, favorable interactions between major groove functional groups and the ligand on the metal might stabilize a more bent structure. It is likely, however, that replacement of the square-planar complex with an octahedral complex would probably prevent further bending of the duplex for steric reasons.

HMG-Domain Protein Binding to Cisplatin-Modified DNA. Many proteins that recognize, bind to, and further bend cisplatin lesions on DNA contain the high mobility group domain.[8] HMG-domain proteins are involved in transcription and bind to specific sequences or unusual structures such as bent DNA or cruciforms. These proteins can bind specifically to and prevent repair of the major cisplatin intrastrand adducts, *cis*-$[Pt(NH_3)_2\{d(GpG)\}]$, and the presumably closely related *cis*-$[Pt(NH_3)_2\{d(ApG)\}]$.[9] Gel electrophoresis studies revealed that HMG-domain protein binding to these lesions increased the overall bend of the DNA from ∼33° to ∼80°.[55] This change in bend angle supports the hypothesis that protein binding might relieve strain at the platinum site by allowing the metal atom to return to a more favorable position in the planes of the guanine bases.

Recently, the solution structures of HMG domains from two proteins, the human testis-determining factor (SRY)[56] and the lymphoid enhancer binding factor (LEF-1),[57] bound to their target DNA sequences, have solved by NMR spectroscopic analysis. The HMG domains from SRY and LEF-1 bind to the minor grooves of their target DNA sequences. In each case, the protein intercalates a hydrophobic residue between two adjacent adenine bases on the target DNA. SRY intercalates an isoleucine (Ile) and LEF-1 inserts a methionine (Met). For both, the protein causes a wedge in the base stack at an AA site from the minor groove side of the helix, effecting a positive

(52) Guan, Y.; Gao, Y.-G.; Liaw, Y.-C.; Robinson, H.; Wang, A. H.-J. *J. Biomol. Struct. Dyn.* **1993**, *11*, 253.
(53) Kozelka, J.; Archer, S.; Petsko, G. A.; Lippard, S. J. *Biopolymers* **1987**, *26*, 1245.
(54) Sandman, K. E.; Lippard, S. J. Unpublished results.
(55) Chow, C. S.; Whitehead, J. P.; Lippard, S. J. *Biochemistry* **1994**, *33*, 15124.
(56) Werner, M. H.; Huth, J. R.; Gronenborn, A. M.; Clore, G. M. *Cell* **1995**, *81*, 705.
(57) Love, J. J.; Li, X.; Case, D. A.; Giese, K.; Grosschedl, R.; Wright, P. E. *Nature* **1995**, *376*, 791. Wright, P. E. Private communication.

Table 6. Comparison of hSRY/DNA and LEF−1/DNA NMR Structures and the Cisplatin/DNA Crystal Structure

	hSRY/DNA[56]	LEF−1/DNA[57]	cisplatin/DNA
DNA form	intermediate A/B	intermediate A/B	junction of A/B
minor groove width (Å)	9.4	11.0 in protein binding region	9.5−11.0
P−P distance (Å)	5.4 Ile intercalation	6.3	5.5 Pt coordination
roll (deg)	19 Ile intercalation	52 Met intercalation	26
average helical twist (deg)	26	32	32
bend: protein/DNA (deg)	∼70−80	∼117	∼80

roll. The positive roll is accompanied by widening of the minor groove and duplex underwinding. In the case of the DNA in the SRY structure, the groove opposite the site of Ile intercalation is 9.4 Å wide, the dihedral angle between the adjacent adenine residues involved in the intercalation is about 19°, and the average helical twist is about 26°. The DNA in the LEF-1 structure has a minor groove width of 11.0 Å, a twist of 19−24° at the site of Met intercalation, and an average helical twist of 32°. The disruption in the double helix caused by intercalation of a side chain from an HMG protein looks similar to that caused by binding of *cis*-$\{Pt(NH_3)_2\}^{2+}$ to adjacent guanine residues on DNA, but a detailed comparison is not possible because the LEF-1 NMR structure coordinates have not yet been released. In the cisplatin−DNA structure, the minor groove opens to a width of about 11.0 Å and the dihedral angle between the planes of the adjacent purines is about 26°. The platinated duplex is also underwound, with an average helical twist of 32°. These values indicate how cisplatin binding can prepare DNA for HMG-domain protein interactions. Some details of the structures of DNA bound to cisplatin and to the HMG domains of SRY and LEF-1 are listed for comparison in Table 6.

Other DNA-Binding Proteins and Bent DNA. DNA binding and bending by proteins have been implicated in biological processes such as transcription. The structure of the TATA binding protein (TBP) complexed with the TATA box illustrates the distinctive bend which a protein can induce in a segment of double helical DNA.[58,59] The DNA bend observed in the TBP/TATA box structure was ∼100° and occurred over four base pairs. The bend did not disrupt base pairing but severely unwound the helix. Another protein which binds to and bends DNA is HIV reverse transcriptase.[60] In the crystal structure of such an adduct, the DNA appeared to be a junction of A-form and B-form DNA with an overall bend of ∼40−45°. This value is very similar to that in the structure of cisplatin-modified DNA and indicates that bent DNA or DNA composed of an A/B junction can be a signal for key biological events.

Concluding Remarks. The crystal structure of the major adduct of cisplatin bound to DNA is an important advance toward understanding how this antitumor drug works. The structure reveals that, because DNA is a remarkably flexible molecule, it can accommodate an intrastrand cisplatin cross-link by adopting an unusual structure. The coordination geometry of the platinum atom and the hydrogen bonding, stacking, and other preferences of the duplex DNA are each modified from their canonical, low-energy form. The resulting bent DNA duplex structure is recognized by proteins which contain the HMG domain. Such recognition may be involved potentiating the anticancer activity of the drug. In order to understand details of the interactions between HMG-domain proteins and cisplatin-modified DNA, the structures of other adducts of the drug on duplex DNA and of protein/platinated−DNA complexes must be solved by X-ray crystallography and NMR spectroscopic analyses. After the basic interactions between HMG-domain proteins and platinated duplex DNA are understood, strategies might be developed rationally to afford more specific protein binding and thereby increase the potency of the drug.

Acknowledgment. This work was supported by Grant CA34992 from the National Cancer Institute. C.A.F. acknowledges support from the Claudia Adams Barr Foundation. We thank Drs. S. F. Bellon and D. P. Bancroft for help with data collection. Professor C. O. Pabo, Professor G. A. Petsko, Dr. A. C. Rosenzweig, and Dr. M. Rould provided guidance during the structure determination. Professors W. K. Olson and H. M. Berman provided helpful information during structure analysis. Professors P. B. Hopkins, A. H.-J. Wang, and P. E. Wright provided coordinates for their NMR structures, and Dr. N. Horton kindly supplied a preprint of ref 47.

Supporting Information Available: Table of water contacts (Table S1); stereo views of the noncrystallographic rotation axis (Figures S1 and S2); stereoview of the superposition of molecules A and B (Figure S3); packing interactions (Figures S4 and S5); views of the A-like and B-like ends of the cisplatin-modified double helix (Figure S6); graphical representations of base pair and base step parameters (Figures S7 and S8); schematic and graphic representations of phosphorus atom distances (Figures S9 and S10); stacking arrangements for the base steps 1−11 (Figure S11−S21) (30 pages). See any masthead page for ordering and Internet access instructions.

JA9625079

(58) Kim, Y.; Geiger, J. H.; Hahn, S.; Sigler, P. B. *Nature* **1993**, *365*, 512.
(59) Kim, J. L.; Nikolov, D. B.; Burley, S. K. *Nature* **1993**, *365*, 520.
(60) Jacobo-Molina, A.; Ding, J.; Nanni, R. G.; Clark, A. D.; Lu, X.; Tantillo, C.; Williams, R. L.; Kamer, G.; Ferris, A. L.; Clark, P.; Hizi, A.; Hughes, S. H.; Arnold, E. *Proc. Natl. Acad. Sci. U.S.A.* **1993**, *90*, 6320.
(61) **Note:** The coordinates for the crystal structure described in this paper have been deposited with the Protein Data Bank and are available under the PDB access code 1GPG or from the authors (lippard@lippard.mit.edu).